Surface-Induced Chirality in a Self-Assembled Monolayer of Discotic Liquid Crystal

Fabrice Charra and Jacques Cousty

Commissariat à l'Énergie Atomique, Direction des Sciences de la Matière, Département de Recherche sur l'État Condensé, les Atomes et les Molécules, Service de Recherche sur les Surfaces et l'Irradiation de la Matière, Centre d'Études de Saclay, F-91191, Gif-sur-Yvette Cedex, France

(Received 2 December 1996; revised manuscript received 24 September 1997)

We report the observation by scanning tunneling microscopy of the emergence of chirality through the self-assembly into monolayers of nonchiral discotic liquid crystals, hexakis-2,3,6,7,10,11-alkyloxytriphenylene, on the nonchiral surface of highly oriented pyrolitic graphite. A chiral ordering transition appears when increasing the triangular aspect ratio of the molecules, through the tuning of alkoxy-side-chain length. The mechanism of this symmetry breaking, which involves steric hindrance, superlattice formation, and conformational mobility, can be understood in the light of a simple frustrated triangular Ising net. [S0031-9007(98)05401-5]

PACS numbers: 68.45.–v, 61.30.Gd, 68.55.–a, 83.70.Jr

Microscopic order in molecular assemblies is known to play a central role in a lot of physical processes. Numerous properties of molecular materials are conditioned by the preservation of some symmetry requirements in their molecular arrangement. Besides its importance in life sciences, chiral asymmetry has considerable consequences on physical properties like optical rotation or optical even-harmonic generation. It is usually achieved by selecting molecules that are themselves chiral, but it can also occur through the chiral ordering of nonchiral molecules. Recently, such chiral phases composed of nonchiral rod-shaped molecules have been observed in Langmuir monolayers [1].

New trends for molecularly designed materials and nanostructures raise the problem of assembling molecules into the required well ordered structure [2]. The self-assembly technique takes advantage of weak intermolecular interactions during thin-film growth in order to achieve a spontaneous organization [2,3]. This requires an accurate knowledge of these forces and of how to control them, either at a molecular level or through external parameters such as substrate-surface interactions. Liquid crystals have provided us with unique models to understand such weak interactions, both as concerns intermolecular forces and molecule-surface forces. Discotic liquid crystals [4] are disk-shaped molecules made of a rigid core surrounded by equatorial flexible chains. They form columnar mesophases where molecular disks stack into columns. They have been observed to form also self-assembled monolayers at liquid-solid interface [5,6].

Scanning tunneling microscopy (STM) has become a major tool to study molecular structure, dynamic and electronic properties of such monolayers, formed on conducting substrates [7–11]. A unique advantage of this technique is the possibility to study local order without averaging over several domains.

In this paper, we report the STM observation of the self-assembled monolayers formed by a series of discotic liquid-crystal molecules on a highly oriented pyrolitic graphite (HOPG) surface. We observe the emergence of a chiral order when increasing the triangular aspect ratio of the molecules, although neither the molecule nor the surface present any chirality. The mechanism of this symmetry breaking, which involves steric hindrance, superlattice formation, and conformational mobility, can be understood in the framework of a simple frustrated triangular Ising net.

Measurements were performed on a Nanoscope II (Digital Instruments) scanning tunneling microscope, with a low-current head. The tunnel current was $I_T = 50$ pA. All images have been recorded in the height (i.e., constant current) mode at a scanning rate of 20 lines per sec, at air and room temperature. We have studied a series of symmetrically 2,3,6,7,10,11-alkoxy-substituted triphenylenes with n-carbon side chains (HnT; see Fig. 1) with $n =$ 5, 7, 9, and 11 [12]. HnT's have been used as highly concentrated, although not saturated (~5 to 20 g/l), solutions in tetradecane (Aldrich, 99%, used as received).

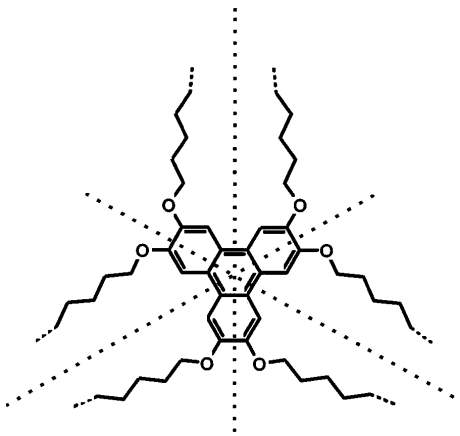

FIG. 1. Molecule of hexakis-2,3,6,7,10,11-alkyloxy-triphenylene which belongs to the D_{3h} point-symmetry group. Dotted lines represent the three in-plane secondary twofold symmetry axes. In the present study, the linear alkyloxy side chains contain 5, 7, 9, and 11 carbons.

 0031-9007/98/80(8)/1682(4)$15.00

Monolayers were prepared on freshly cleaved HOPG (Le Carbone Lorraine, France). Both the solution and the substrate were gently heated up to 45–55 °C. Then, a drop of the solution was applied to HOPG and quenched down to room temperature within a few minutes. A mechanically cut 80:20-platinum-iridium STM tip was then immersed into the solution in order to image the self-assembled layer formed spontaneously at the liquid-solid interface.

All four molecules form layers highly reproducible through this procedure, with domains larger than 100 nm. The STM images that we report here are typical ones, which have been repeatedly observed.

At sample tunnel voltages of $V_S = -1.8$ to -1.4 V, molecules are imaged as bright spots which can be attributed to aromatic cores since conjugated π-electron systems are known to give large contributions to STM images [13–15]. The lattices appear then clearly [Figs. 2(a)–2(d)]. Similarly to columnar mesophases, the two-dimensional lattices observed here are hexagonal. In the case of H7T, however, the hexagonal lattice is slightly distorted [Fig. 2(b)] with a column pairing consistent with earlier observations [6].

The distance between nearest-neighbor molecules increases progressively from 1.78 nm for H5T layers up to 2.28 nm for H11T but is always smaller than the distance between columns in corresponding 3D mesophase (2.02 to 2.56 nm from H5T to H11T [16]). This indicates densely packed layers with an increased lateral intermolecular interaction compared to the columnar phase. In some instances, we have been able to observe simultaneously the molecular layer and the HOPG surface in uncovered regions at domain boundaries. This proves that the liquid-solid interface observed consists in one monomolecular layer. Remarkably, Figs. 2(a)–2(d) reveal the appearance of a superlattice for molecules with longer side chains: Every third molecule appears brighter in H9T and H11T layers, whereas all molecules are equivalent for H5T and H7T ones. Brighter molecules in H9T and H11T form a $\sqrt{3} \times \sqrt{3}\,\mathrm{R}30°$ superlattice with overall lattice constants $a = 3.75$ and 3.95 nm, respectively. Another noticeable difference between short- and long-side-chain molecules is that intramolecular resolution can be achieved for $n \geq 9$, as shown in Fig. 3, while H5T molecules are always imaged as simple disks for all tested bias varying from -1.8 to 1.8 V. Both the distances between conjugated cores and the hexagonal lattice suggest that all molecules rest flat on HOPG. This is supported, for H9T and H11T,

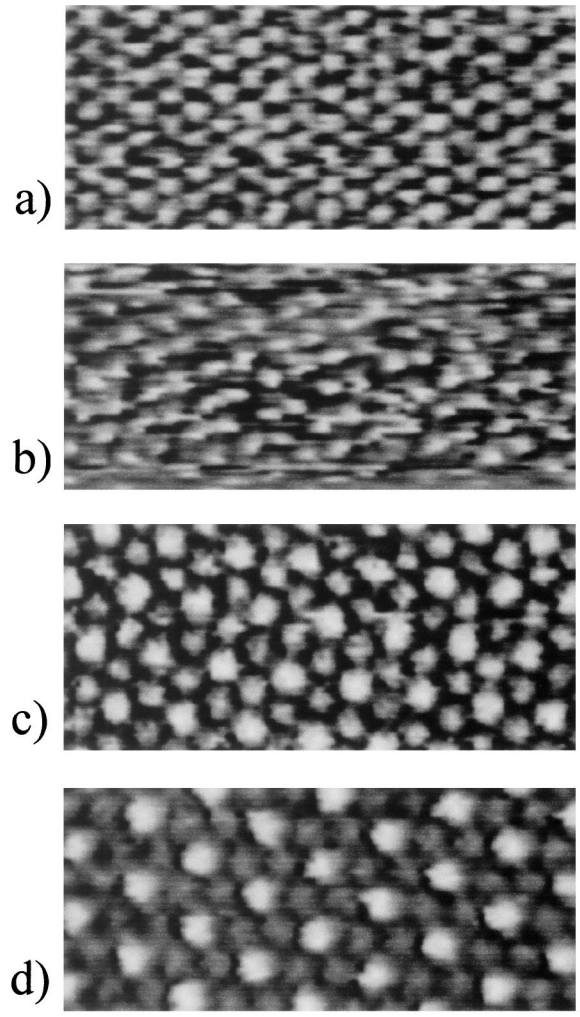

FIG. 2. STM images (29 × 13 nm) of single domains of HnT monolayers, at the interface between graphite and a tetradecane solution. (a) H5T, $V_S = +1400$ mV; (b) H7T, $V_S = +1700$ mV; (c) H9T, $V_S = +1800$ mV; (d) H11T, $V_S = +1800$ mV. The tunnel current is 50 pA for all images.

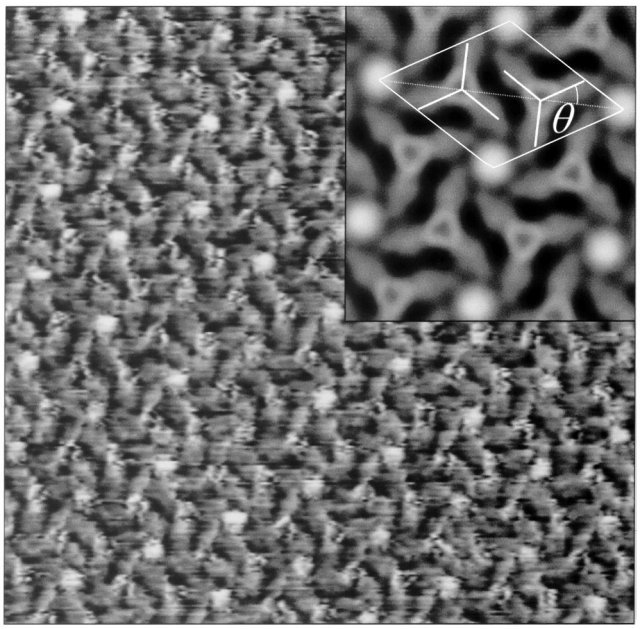

FIG. 3. High-resolution STM image (29 × 28 nm) of a H11T monolayer at $V_S = +350$ mV. Z scale = 2.2 Å. The inset shows the corresponding symmetrized correlation averaged image. The unit cell is represented and the angle θ between (1,1) lattice direction (dotted line) and presumed twofold molecular axis (solid segments) is displayed.

by some high-resolution images where all conjugated cores appear as identical rings, with radii ~0.35 nm corresponding to a maximum height located nearly above most external carbon atoms of the aromatic moiety. Furthermore, some cores are clearly surrounded by three wings that can be identified with the three side-chain pairs of H11T. In the following, we focus on the case of longer side chains ($n \geq 9$) prototyped by H11T. Two types of sites can be distinguished in Fig. 3: Two molecules are in sites with C_3 symmetry, the third molecule, the brighter one in Figs. 2(c) and 2(d), appearing in a site with C_6 symmetry. The two C_3 sites can be deduced one from another by a 60° rotation around the center of the C_6 site. The resulting sixfold symmetry of the overall system is confirmed by Fourier-transform analysis and the above structure appears more clearly in the correlation-averaged and symmetrized image of the unit cell reported as an inset in Fig. 3. In the latter, some geometry elements of the single H11T molecule in C_3 sites can be identified. They are also discernible in the untreated image. The three in-plane secondary twofold axes of the molecules can then be deduced. They form a $\theta \sim 30°$ angle with respect to the corresponding C_3-C_6 axis [i.e., the (1,1) direction; see inset in Fig. 3]. As a consequence of this nonzero (mod 60°) θ angle, both C_3 sites present a chiral asymmetry. Since, in a given domain, all such sites pertain to the same left- or right-handed chiral orientation, the whole domain structure is chiral. As expected since neither single molecules nor HOPG are chiral, two kinds of domains with left- and right-handed structures are readily statistically equally observed.

Whereas the side chains of molecules in C_3 sites are resolved, no preferred orientation can be evidenced for the molecule in C_6 sites. Moreover, the appearing C_6 symmetry corresponds to an increase compared with the threefold symmetry of the D_{3h} single molecule. We can thus infer that molecules in C_6 sites possess a rotational degree of freedom which enables alternation between at least two configurations rotated by 60°, at a rate faster than STM scanning. This orientational mobility, which is common to all molecules in the bulk columnar phase, confers a mesophase character to the monolayer.

These structures can be interpreted within the framework of a frustrated antiferromagneticlike triangular Ising net, as sketched in Fig. 4. In the limit case of pure discotic (C_∞) molecules the larger coverage corresponds to a triangular lattice, each molecule lying within a hexagonal site with a free rotational degree of freedom. This is the case for 3D columnar mesophases of triphenylenes [4]. Now, considering molecules with an increasingly pronounced triangular shape, one expects such molecules to have two preferred orientations within their hexagonal sites, as sketched in Fig. 4 (denoted u and d). Moreover, because of steric hindrance, the mutual interaction energy experienced by two neighboring molecules will favor antiparallel orientation. This antiferromagneticlike coupling

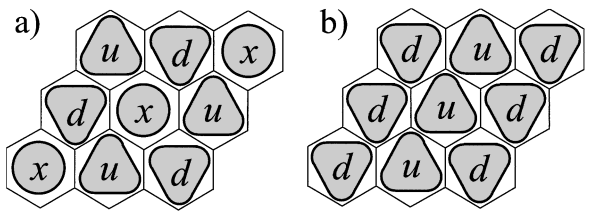

FIG. 4. Schematic representation of two configurations with the lowest possible energy of the antiferromagneticlike triangular Ising net described in the text. u and d represent the two preferred orientations of the triangular molecules in their hexagonal sites. x represents a molecule with random orientation. (a) Chiral configuration ascribed to H9T and H11T monolayers; (b) nonchiral configuration ascribed to H7T. The *low-coupling* or *high-temperature* configuration ascribed to H5T corresponds to the all-x structure (not represented).

can be modelized by a model Ising Hamiltonian H representing the interaction between every site α, with orientation $S_\alpha = +1$ or -1 for u and d states, and its six nearest neighbors β:

$$H = -J \sum_\alpha \left(\sum_\beta S_\alpha S_\beta \right), \quad \text{with } J < 0 .$$

Such an antiferromagnetic triangular Ising net has been extensively studied as a model case of frustrated system [17]. The different structures observed for HnT monolayers can be directly identified with the phases predicted for the model Ising system schematized in Fig. 4 (u and d labels). The $\sqrt{3} \times \sqrt{3}$ superstructure observed for both H9T and H11T on one hand and the 2×1-like superstructure observed for H7T on the other hand, correspond to the two lowest-energy structures ($\langle E \rangle = 2J$ per site) extrapolated from the Ising Z-spin model [17]. The $\sqrt{3} \times \sqrt{3}$ structure is favored by a finite entropy through the random orientation of every third molecule. Unlike in the Z-spin Ising system, the system of threefold symmetry molecules exhibits centrosymmetry breaking in the $\sqrt{3} \times \sqrt{3}$ structure. More precisely, this structure is chiral and changes between left- and right-handed configurations through u-d reversal of all molecules. The disordered phase of H5T corresponds to the case of low coupling coefficients $|J|$ or high temperature T. Hence the increase of side-chain length yields a subsequent increase of the coupling coefficient $|J|$. The existence of the low-energy 2×1-like superstructure for H7T, i.e., as a transition between the two limit phases, is unexpected from entropy considerations. Remarkably, a similar situation has been predicted for Langmuir monolayers and smectic films composed of rod-shaped molecules, stripe patterns being formed between a high-temperature uniform nonchiral phase and a low-temperature uniform chiral phase [18].

With slightly different triphenylene derivatives, a $\sqrt{3} \times \sqrt{3}\,\mathrm{R}30°$ superlattice has been observed in the column arrangement of a particular mesophase (D_{ho}) [19], the true nature of which is still an open question. The same

rearrangement observed here for the two-dimensional phase substantiates the coupled Ising model proposed for the three-dimensional D_{ho} phase [20]. In this latter case, every third column is displaced by half an intermolecular intracolumnar distance in the vertical direction. A similar displacement probably occurs in the two-dimensional array studied here, which could explain the differences in STM imaging properties of the molecule in the C_6 site compared with the other two molecules of the unit cell.

It is also to be noticed that, although isolated H*n*T molecules are not chiral, they can adopt a chiral conformation when they occupy chiral C_3 and C_6 sites. Analysis of epitaxial relations between the molecular layer and HOPG supports this hypothesis and will be reported elsewhere.

These observations raise numerous further questions on the control of this surface-induced chirality through molecular, surface, or other external parameters. For example, one could expect that the use of modified chiral molecules would favor one domain orientation compared to its mirror symmetric. This would be manifested by unbalanced proportion of domain orientations when using a nonracemic mixture, or a segregation of stereoisomers into different domains when using a racemic mixture. Another major question is whether the surface-induced chirality can propagate into the bulk during a layer-by-layer growth.

We are highly grateful to Helmut Ringsdorf and Holger Bengs from University of Mainz (Germany) for providing us with high-purity hexakisalkyloxy-triphenylenes. We are also much indebted to Dimitra Markovitsi from CNRS in Saclay (France) for fruitful discussions and suggestions.

[1] R. Viswanathan, J. A. Zasadzinski, and D. K. Schwartz, Nature (London) **368**, 440 (1994).
[2] W. M. Tolles, in *Nanotechnology*, edited by G. M. Chow and K. E. Gonsalves, ACS Symposium Series Vol. 622 (American Chemical Society, Washington, DC, 1996), Chap. 1.
[3] R. H. Tredgold, *Order in Thin Organic Films* (Cambridge University Press, Cambridge, England, 1994), Chap. 6.
[4] A. M. Levelut, J. Chim. Phys. **80**, 149 (1983).
[5] J. P. Rabe, S. Buchholz, and L. Askadskaya, Synth. Met. **54**, 339 (1993).
[6] L. Askadskaya, C. Boeffel, and J. P. Rabe, Ber. Bunsen-Ges. Phys. Chem. **97**, 517 (1993).
[7] G. C. McGonigal, R. H. Bernhardt, and D. J. Thomson, Appl. Phys. Lett. **57**, 28 (1990).
[8] G. C. McGonigal, R. H. Bernhardt, Y. H. Yeo, and D. J. Thomson, J. Vac. Sci. Technol. B **9**, 1107 (1991).
[9] J. P. Rabe and S. Buckholz, Phys. Rev. Lett. **66**, 2096 (1991).
[10] J. P. Rabe and S. Buckholz, Science **253**, 424 (1991).
[11] G. Watel, F. Thibaudau, and J. Cousty, Surf. Sci. **281**, L297 (1993).
[12] W. Kranig, B. Hüser, H. W. Spiess, W. Kreuder, H. Ringsdorf, and H. Zimmerman, Adv. Mater. **2**, 36 (1990).
[13] D. P. E. Smith, J. K. H. Hörber, G. Binnig, and H. Nejoh, Nature (London) **344**, 641 (1990).
[14] P. Sautet and C. Joachim, Chem. Phys. Lett. **185**, 23 (1991).
[15] J. Fisher and P. E. Blöchl, Phys. Rev. Lett. **70**, 3263 (1993).
[16] D. Markovitsi, A. Germain, P. Millié, P. Lécuyer, L. K. Gallos, P. Argyrakis, H. Bengs, and H. Ringsdorf, J. Phys. Chem. **99**, 1005 (1995).
[17] G. H. Wannier, Phys. Rev. **79**, 357 (1950).
[18] J. V. Selinger, Z. G. Wang, R. F. Bruinsma, and C. M. Knobler, Phys. Rev. Lett. **70**, 1139 (1993).
[19] E. Fontes, P. A. Heiney, and W. H. de Jeu, Phys. Rev. Lett. **61**, 1202 (1988).
[20] M. Hérbert and A. Caillé, Phys. Rev. E **51**, R1651 (1995).